

Research Article

Free Vibration Analysis of Thick Rectangular and Elliptical Plates with Concentric Cut-Out

Anjibabu Merneedi ¹, Nalluri Mohan Rao,² L. Natrayan ,³ L. Yuvaraj ,⁴
and Prabhu Paramasivam ⁵

¹Department of Mechanical Engineering, Aditya College of Engineering, Surampalem 533437, Andhra Pradesh, India

²Department of Mechanical Engineering, University College of Engineering, JNTUK, Kakinada 533003, India

³Department of Mechanical Engineering, Saveetha School of Engineering, SIMATS, Chennai 602105, Tamil Nadu, India

⁴Department of Automobile Engineering, Acharya Institute of Technology, Bangalore 560107, Karnataka, India

⁵Department of Mechanical Engineering, College of Engineering and Technology, Mettu University, Metu 318, Ethiopia

Correspondence should be addressed to Anjibabu Merneedi; anjiamiable@gmail.com and L. Natrayan; natrayanphd@gmail.com

Received 24 June 2021; Revised 11 July 2021; Accepted 21 September 2021; Published 16 October 2021

Academic Editor: Samson Jerold Samuel Chelladurai

Copyright © 2021 Anjibabu Merneedi et al. This is an open access article distributed under the Creative Commons Attribution License, which permits unrestricted use, distribution, and reproduction in any medium, provided the original work is properly cited.

This research paper deals with a numerical method which is modified and applied, by the authors to derive an eigenvalue of a thick plate having cut-out in which geometries of plate and cut-outs are different, through a deflection matching condition by including shear deformation and rotary inertia effects, with less computational efforts and high accuracy. The modified Independent Coordinate Coupling Method (ICCM) is validated with FEM package (ANSYS) and applied to know the change in eigenvalues for a plate with cut-out by varying various parameters like aspect ratios, cut-out size, and thickness ratios. Trigonometric functions considered at the boundary level conditions of a simply supported plate should be satisfied. Free vibrational exploration on a thick isotropic plate with various aspect ratios and an elliptical plate with various sizes is carried out through the modified ICCM. Independent coordinates are applied for a plate domain and for a hole domain individually followed by equating the deflection condition of hole and plate, a reduced mass to express with cut-out from which eigenvalues can be obtained. The deflection matching condition facilitates the analysis even though the geometries of plate and cut-outs are different.

1. Introduction

A plate with a cut-out is a commonly existing structure in the domain of aeronautics, civil, marine, and mechanical engineering to accommodate mountings or accessories under the action of various forces. In dealing with such cases, knowledge on dynamics of plates plays a vital role. Plates with cut-outs are subjected to free vibration. Eigenvalues of thin plates may be calculated using classical plate theory and easily obtained, whereas they cannot be applied directly in thick plate analysis due to the effect of rotary inertia. This leads to an overestimation of results. The expression of strain and potential energies of plate must contain the terms of shear and rotary inertia to improve the accuracy of eigenvalues while computing.

From the literature available on the Mindlin plates, Senjanovic et al. [1, 2] derived exact formulas for a plate by reducing a

three-equation system to one equation expressing a potential function in terms of bending deflection. Xiang et al. [3] analyzed Mindlin plates by implementing delta type of kernel wavelet in lateral vibration of plates. Merneedi et al. [4, 5] applied the ICCM method of elliptical and rectangular thin plate by changing the size, position, and number of holes at all possible ways. Aksu [6] applied an energy approach along with a finite difference in a Mindlin's dynamic analysis approach of plate having cut-outs. Rui et al. [7] applied a rational method of superposition in the symplectic space for Mindlin plate's vibration analysis. Xing and Liu [8, 9], implemented a new two-eigenfunction theory to obtain vibrational solutions of a rectangular Mindlin plate, in which amplitude and generalized curvatures are considered as functions.

Liew et al. [10–13] minimized energy function of Mindlin's theory by using the Rayleigh–Ritz method to formulate the

governing eigenvalue equations. Dawe and Roufaeil [14] derived by assuming that plate deflection and rotations are a sequence. The Rayleigh–Ritz approach may be used to compute the natural frequencies of flexural vibrations of a square plate using products of appropriate Timoshenko beam functions. Leissa [15, 16] investigates the free vibrational exploration for twenty-one cases of various rectangular plates through precise analytical techniques. Sayyad and Ghugal [17], proposed a displacement-based theory in which thickness coordinates are used as an exponential function so that transverse shear stress can be obtained directly without any shear correction factor. Kanak and Salil [18] and Merneedi et al. [5] consider the nine-node isoparametric element. The natural frequencies of thin and thick plates with cut-outs were analysed using the first-order shear deformation theory. Prasad et al. [19] utilized the Rayleigh–Ritz approach to apply a three-term deflection function on clamped and simply supported elliptical plates. Leissa [20] calculated the precise fundamental natural frequencies of a simple sup. Maurizi et al. [21], derived fundamental natural frequencies for a vibration of elastic plate using simple static in the presence of a clamped boundary condition. Lam et al. [22] created a computational tool to determine the natural frequencies of circular and elliptical plates; the researchers used the Rayleigh–Ritz method using a set of orthogonal functions called acceptable functions. Shibaoka [23] creates a fundamental normal mode of flexural vibration of an elliptical plate under clamped-clamped boundary conditions. Mcnitt [24] utilized the Galerkin method and an ordinary product solution by ignoring the impact of rotational inertia in the investigation of free vibration of an elliptical plate under clamped boundary conditions using traditional small-deflection theory. Kwak and Han [25] used ICCM to do a free vibrational exploration on a rectangular plate with a hole obtaining energy linked to the hole with plate separately and equated by matching condition of deflection. Hasheminejad et al. [26] formulated the analytical expression for the elliptical plate with an eccentric cut-out. The solution is derived using Helmholtz's decomposition theorem, and this technique is based on Navier's displacement equation of motion. Mathieu functions of translational addition theorems are used to separate the variables.

According to the literature, eigenvalues of a thick rectangular plate with a hole were estimated using several numerical tools such as the Rayleigh–Ritz methodology, FEM, and finite difference techniques and the plate is same. It is identified that if hole and plate are of different geometries, the RRM may lead to complex integrals with tedious numerical computations because of its integral limits [27]. Keeping in view of this, in the present work, the authors proposed a novel modified ICCM to determine the natural frequencies of a structure with cut-out of different shapes by implementing a deflection matching condition along with closed-form integrals to reduce the computational efforts. Shear deformation and rotational inertia effects are among them. Even if the shape of the plate and hole differs, the deflection matching condition simplifies the analysis, which is a key benefit of the ICCM. Using the ICCM, a Mindlin elliptical and rectangular plate's first six natural frequencies with various sizes of cut-outs under simply supported boundary conditions were derived to show the variation of natural frequencies with respect to various hole sizes, and the same is validated through ANSYS software including mode shapes, which was not covered in the literature in view of the authors.

1.1. Free Vibrational Exploration of Rectangle Plate with Cut-Out. Separate energy expressions are formulated for a hole domain and for a plate domain exploration of a plate with hole, and hence deflection matching condition is essential to establish a kinematic relation between these independent coordinate domains. It will also enable us to unify these two independent energies.

1.1.1. Expressions for Rectangular Plate. Consider a thick rectangular plate with a cut-out in $x - y$ plane, having dimensions of $a \times b$ and $a_c \times b_c$, respectively. Expressions for rectangular plate strain energy and kinetic energy from Reference [11] are as follows:

$$V_p = \frac{1}{2} \int_v \left\{ \frac{Eh^2}{1-\mu^2} \left[\left(\frac{\partial \psi_x}{\partial x} + \frac{\partial \psi_y}{\partial y} \right)^2 - 2(1-\mu) \left(\frac{\partial \psi_x}{\partial x} \frac{\partial \psi_y}{\partial y} - \frac{1}{4} \left(\frac{\partial \psi_x}{\partial y} + \frac{\partial \psi_y}{\partial x} \right)^2 \right) \right] + \kappa G \left[\left(\psi_x + \frac{\partial w}{\partial x} \right)^2 + \left(\psi_y + \frac{\partial w}{\partial y} \right)^2 \right] \right\} dv,$$

$$T_p = \frac{1}{2} \omega^2 \int_A \left[\rho h w^2 + \frac{1}{12} \rho h^3 (\psi_x^2 + \psi_y^2) \right] dA,$$
(1)

where h = plate thickness, ρ = mass density, E = modulus of elasticity, w = transverse displacement, G = shear modulus, μ = Poisson's ratio, $\psi_x = -\partial w / \partial x$ = rotation about y direction, $\psi_y = -\partial w / \partial y$ = rotation about x direction, κ = shear correction factor = 5/6, and ω = angular frequency.

Introducing a non-dimensional parameter, thickness to width ratio $\beta = h/b$, aspect ratio $\alpha = a/b$, and non-dimensional variables $\xi = x/a$, $\eta = y/b$, the energy expression of plate is a non-dimensional representation of plate which can be written as follows:

$$V_p = \int_0^1 \int_0^1 \left\{ \left(\frac{1}{\alpha} \frac{\partial \psi_x}{\partial \xi} + \frac{\partial \psi_y}{\partial \eta} \right)^2 - 2(1-\mu) \left[\frac{1}{\alpha} \frac{\partial \psi_x}{\partial \xi} \frac{\partial \psi_y}{\partial \eta} - \frac{1}{4} \left(\frac{\partial \psi_x}{\partial \eta} + \frac{1}{\alpha} \frac{\partial \psi_y}{\partial \xi} \right)^2 \right] \right. \\ \left. + \frac{6(1-\mu)\kappa}{\beta^2} \left[\left(\psi_x + \frac{1}{\alpha} \frac{\partial w}{\partial \xi} \right)^2 + \left(\psi_y + \frac{\partial w}{\partial \eta} \right)^2 \right] \right\} abd\xi d\eta, \quad (2a)$$

$$T_p = \int_0^1 \int_0^1 \left[w^{*2} + \frac{1}{12} \beta^2 (\psi_x^2 + \psi_y^2) \right] abd\xi d\eta, \quad (2b)$$

where $w^* = w/b$.

Admissible functions are considered to expand transverse deflection and the rotations in equations (2a) and (2b) as

$$\begin{aligned} w(\xi, \eta, t) &= \bar{A}_i(\xi, \eta)\Omega(t), \\ \psi_x(\xi, \eta, t) &= \bar{B}_i(\xi, \eta)\Omega(t), \\ \psi_y(\xi, \eta, t) &= \bar{C}_i(\xi, \eta)\Omega(t), \end{aligned} \quad (3)$$

where $\bar{A}_i(\xi, \eta) = [A_1 \ A_2 \ A_3 \ A_4 \ \dots \ A_m]$ is a $(1 \times m)$ matrix and $\Omega_i(\xi, \eta) = [\Omega_1 \ \Omega_2 \ \Omega_3 \ \Omega_4 \ \dots \ \Omega_m]^T$ is $(m \times 1)$ generalized coordinate vector, where “m” denotes admissible functions required for the approximating the deflection curve.

Substituting equation (3) in equations (2a) and (2b) yields

$$T_p = \frac{1}{2} \dot{\Omega}^T M \dot{\Omega}, \quad (4a)$$

$$V_p = \frac{1}{2} \Omega^T K \Omega, \quad (4b)$$

in which

$$M = \rho h b^2 \bar{M}, \quad (5a)$$

$$K = \left(\frac{D}{b^2} \right) \bar{K}, \quad (5b)$$

where

$$\bar{M} = \int_0^1 \int_0^1 \left[(\bar{A}^T \cdot \bar{A}) + \frac{\beta^2}{12} (\bar{B}^T \cdot \bar{B} + \bar{C}^T \cdot \bar{C}) \right] d\xi d\eta, \quad (6a)$$

$$\bar{K} = \int_0^1 \int_0^1 \left\{ \begin{aligned} & \left[\frac{1}{\alpha^2} \frac{\partial \bar{B}^T}{\partial \xi} \cdot \frac{\partial \bar{B}}{\partial \xi} + \frac{\partial \bar{C}^T}{\partial \eta} \cdot \frac{\partial \bar{C}}{\partial \eta} + \frac{1}{\alpha} \left[\frac{\partial \bar{B}^T}{\partial \xi} \cdot \frac{\partial \bar{C}}{\partial \eta} + \frac{\partial \bar{C}^T}{\partial \eta} \cdot \frac{\partial \bar{B}}{\partial \xi} \right] \right] + \\ & (1-\mu) \cdot \left[\frac{1}{\alpha} \left[\frac{\partial \bar{B}^T}{\partial \xi} \cdot \frac{\partial \bar{C}}{\partial \eta} + \frac{\partial \bar{C}^T}{\partial \eta} \cdot \frac{\partial \bar{B}}{\partial \xi} \right] - \frac{1}{2} \left[\left[\frac{\partial \bar{B}^T}{\partial \eta} \cdot \frac{\partial \bar{B}}{\partial \eta} + \frac{1}{\alpha^2} \frac{\partial \bar{C}^T}{\partial \xi} \cdot \frac{\partial \bar{C}}{\partial \xi} \right] + \frac{1}{\alpha} \left[\frac{\partial \bar{B}^T}{\partial \eta} \cdot \frac{\partial \bar{C}}{\partial \xi} + \frac{\partial \bar{C}^T}{\partial \xi} \cdot \frac{\partial \bar{B}}{\partial \eta} \right] \right] \right] + \\ & \left[\frac{6(1-\mu)\kappa}{\beta^2} \left[\left[\bar{B}^T \cdot \bar{B} + \frac{1}{\alpha^2} \frac{\partial \bar{A}^T}{\partial \xi} \cdot \frac{\partial \bar{A}}{\partial \xi} + \frac{1}{\alpha} \left[\bar{B}^T \cdot \frac{\partial \bar{A}}{\partial \xi} + \frac{\partial \bar{A}^T}{\partial \xi} \cdot \bar{B} \right] \right] + \left[\bar{C}^T \cdot \bar{C} + \frac{\partial \bar{A}^T}{\partial \eta} \cdot \frac{\partial \bar{A}}{\partial \eta} + \bar{C}^T \cdot \frac{\partial \bar{A}}{\partial \eta} + \frac{\partial \bar{A}^T}{\partial \eta} \cdot \bar{C} \right] \right] \right] \end{aligned} \right\} d\xi d\eta. \quad (6b)$$

In equations (6a) and (6b), stiffness matrices are represented by \bar{M} , \bar{K} , respectively, along with non-dimensional variables. Equation of motion of plate is obtained by substituting equation (3) in Lagrange’s expression, and its eigenvalue can be computed from

$$[K - \omega^2 M] \Lambda = 0. \quad (7)$$

Using non-dimensional matrices introduced in equations (4a) and (4b), the above eigenvalue problem in non-dimensional form

$$[\bar{K} - \bar{\omega}^2 \bar{M}] \Lambda = 0 \quad (8)$$

will give non-dimensional eigenvalues of a plate, in which “ Λ ” is an eigenvector. In equation (7),

$$\bar{\omega} = \left(\frac{\omega b^2}{\pi^2} \right) \sqrt{\frac{\rho h}{D}} \quad (9)$$

is known as the frequency parameter which represents the flexural rigidity in $D = Eh^3/12(1-\mu^2)$, which is known.

To obtain in terms of admissible function matrices in the X and Y directions, an admissible function matrix from equation (3) has to be changed.

$$\begin{aligned}\bar{A}_i(\xi, \eta) &= A_i(\xi)a_i(\eta), \\ \bar{B}_i(\xi, \eta) &= B_i(\xi)b_i(\eta), \\ \bar{C}_i(\xi, \eta) &= C_i(\xi)c_i(\eta),\end{aligned}\quad (10)$$

where, $i = 1, 2, 3 \dots m$.

1.1.2. Boundary Conditions. A thick simply supported plate is considered and its eigenvalues are derived by considering an individual eigenfunction in each direction for each admissible function.

$$\begin{aligned}A_i(\xi) &= \sqrt{2} \sin(i\pi\xi), \\ a_i(\eta) &= \sqrt{2} \sin(i\pi\eta), \\ B_i(\xi) &= \sqrt{2} \cos(i\pi\xi), \\ b_i(\eta) &= \sqrt{2} \sin(i\pi\eta), \\ C_i(\xi) &= \sqrt{2} \sin(i\pi\xi), \\ c_i(\eta) &= \sqrt{2} \cos(i\pi\eta).\end{aligned}\quad (11)$$

Admissible functions in equation (11) are taken into account in such a way that they meet the assumed boundary conditions of the plate. All geometrical end points of (ξ, η) in equation (3) along with equation (11) will result in a zero deflection.

1.1.3. Energy Expressions for Rectangular Plate with Cut-Out Using ICCM. Kinematic relations are formulated for a plate having cut-out using ICCM; by matching the plate's deflection to the hole's deflection, these relationships may be used to produce updated mass and stiffness matrices as well as distinct plate and hole domains having their own coordinates. Fixing local coordinates to the hole domain is presented for rectangular hole in rectangular plate as illustrated in Figure 1.

Taking non-dimensional coordinates into account, displacement and rotations are expressed as $\xi_h = x_c/a_c$ and $\eta_h = y_c/b_c$.

$$\begin{aligned}w_h(\xi_h, \eta_h, t) &= \bar{A}_{hi}(\xi_h, \eta_h)\Omega(t), \\ \psi_{hx}(\xi_h, \eta_h, t) &= \bar{B}_{hi}(\xi_h, \eta_h)\Omega(t), \\ \psi_{hy}(\xi_h, \eta_h, t) &= \bar{C}_{hi}(\xi_h, \eta_h)\Omega(t),\end{aligned}\quad (12)$$

where $\bar{A}_{hi}(\xi_h, \eta_h) = [A_{h1} \ A_{h2} \ A_{h3} \ \dots \ A_{hm}]$ is an $(1 \times m_h)$ function matrix and $\Omega_h(t) = [\Omega_{h1} \ \Omega_{h2} \ \Omega_{h3} \ \dots \ \Omega_{hm}]^T$ is a $(m_h \times 1)$, here " m_h " is the number of acceptable functions used to approximate deflection in a generalized coordinate vector.

$$\begin{aligned}\bar{A}_{hi}(\xi_h, \eta_h) &= A_{hi}(\xi_h)a_{hi}(\eta_h), \\ \bar{B}_{hi}(\xi_h, \eta_h) &= B_{hi}(\xi_h)b_{hi}(\eta_h), \\ \bar{C}_{hi}(\xi_h, \eta_h) &= C_{hi}(\xi_h)c_{hi}(\eta_h), \\ \text{where, } i &= 1, 2, 3, \dots m_h.\end{aligned}\quad (13)$$

Equations (12) and (13) represented the potential and kinetic energies.

$$T_H = \frac{1}{2} \dot{\Omega}_h^T M_h \dot{\Omega}_h, \quad (14a)$$

$$V_H = \frac{1}{2} \Omega_h^T K_h \Omega_h. \quad (14b)$$

Hence, total energies of plate with hole are

$$T_{\text{total}} = \frac{1}{2} \dot{\Omega}^T M \dot{\Omega} - \frac{1}{2} \dot{\Omega}_h^T M_h \dot{\Omega}_h, \quad (15a)$$

$$V_{\text{total}} = \frac{1}{2} \Omega^T K \Omega - \frac{1}{2} \Omega_h^T K_h \Omega_h, \quad (15b)$$

where

$$\begin{aligned}M_h &= \rho h b_c^2 \bar{M}_h, \\ K_h &= \left(\frac{D}{b_c^2}\right) \bar{K}_h,\end{aligned}\quad (16)$$

in which

$$\bar{M}_h = \int_0^1 \int_0^1 \left[(\bar{A}_h^T \cdot \bar{A}_h) + \frac{\beta_c^2}{12} (\bar{B}_h^T \cdot \bar{B}_h + \bar{C}_h^T \cdot \bar{C}_h) \right] d\xi_h d\eta_h, \quad (17)$$

$$\bar{K}_h = \int_0^1 \int_0^1 \left\{ \begin{aligned} & \left[\frac{1}{\alpha_c^2} \frac{\partial \bar{B}_h^T}{\partial \xi_h} \cdot \frac{\partial \bar{B}_h}{\partial \xi_h} + \frac{\partial \bar{C}_h^T}{\partial \eta_h} \cdot \frac{\partial \bar{C}_h}{\partial \eta_h} + \frac{1}{\alpha_c} \left[\frac{\partial \bar{B}_h^T}{\partial \xi_h} \cdot \frac{\partial \bar{C}_h}{\partial \eta_h} + \frac{\partial \bar{C}_h^T}{\partial \eta_h} \cdot \frac{\partial \bar{B}_h}{\partial \xi_h} \right] \right] + \\ & (1 - \mu) \cdot \left[\frac{1}{\alpha_c} \left[\frac{\partial \bar{B}_h^T}{\partial \xi_h} \cdot \frac{\partial \bar{C}_h}{\partial \eta_h} + \frac{\partial \bar{C}_h^T}{\partial \eta_h} \cdot \frac{\partial \bar{B}_h}{\partial \xi_h} \right] - \frac{1}{2} \left[\left[\frac{\partial \bar{B}_h^T}{\partial \eta_h} \cdot \frac{\partial \bar{B}_h}{\partial \eta_h} + \frac{1}{\alpha_c^2} \frac{\partial \bar{C}_h^T}{\partial \xi_h} \cdot \frac{\partial \bar{C}_h}{\partial \xi_h} \right] + \frac{1}{\alpha_c} \left[\frac{\partial \bar{B}_h^T}{\partial \eta_h} \cdot \frac{\partial \bar{C}_h}{\partial \xi_h} + \frac{\partial \bar{C}_h^T}{\partial \xi_h} \cdot \frac{\partial \bar{B}_h}{\partial \eta_h} \right] \right] \right] + \\ & \left[\frac{6(1-\mu)\kappa}{\beta_c^2} \left[\left[\bar{B}_h^T \cdot \bar{B}_h + \frac{1}{\alpha_c^2} \frac{\partial \bar{A}_h^T}{\partial \xi_h} \cdot \frac{\partial \bar{A}_h}{\partial \xi_h} + \frac{1}{\alpha_c} \left[\bar{B}_h^T \cdot \frac{\partial \bar{A}_h}{\partial \xi_h} + \frac{\partial \bar{A}_h^T}{\partial \xi_h} \cdot \bar{B}_h \right] \right] \right] + \left[\bar{C}_h^T \cdot \bar{C}_h + \frac{\partial \bar{A}_h^T}{\partial \eta_h} \cdot \frac{\partial \bar{A}_h}{\partial \eta_h} + \bar{C}_h^T \cdot \frac{\partial \bar{A}_h}{\partial \eta_h} + \frac{\partial \bar{A}_h^T}{\partial \eta_h} \cdot \bar{C}_h \right] \right] \end{aligned} \right\} d\xi_h d\eta_h, \quad (18)$$

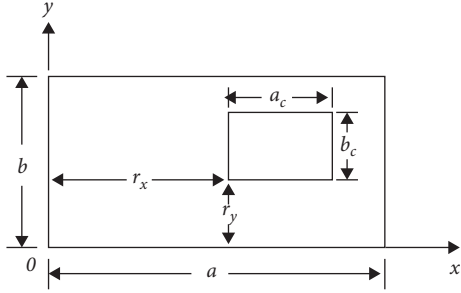


FIGURE 1: Rectangular plate opening with cut-out.

where thickness to width ratio $\beta_c = h/b_c$, aspect ratio $\alpha_c = a_c/b_c$, and non-dimensional variables $\xi_h = x_c/a_c$ and $\eta_h = y_c/b_c$.

Equations (17) and (18) have a distinctive advantage that the integral bounds range from 0 to 1, allowing for a closed-form solution. In terms of plate domain, the displacement

$$\begin{aligned} \sum_{i=1}^{m_h} \bar{A}_{hi}(\xi_h, \eta_h) \bar{B}_{hi}(\xi_h, \eta_h) \bar{C}_{hi}(\xi_h, \eta_h) \Omega_{hi}(t) &= \sum_{i=1}^{m_h} A_{hi}(\xi_h) a_{hi}(\eta_h) B_{hi}(\xi_h) b_{hi}(\eta_h) C_{hi}(\xi_h) c_{hi}(\eta_h) \Omega_{hi}(t) \\ &= \sum_{k=1}^m \bar{A}_k(\xi, \eta) \bar{B}_k(\xi, \eta) \bar{C}_k(\xi, \eta) \Omega_k(t) \\ &= \sum_{k=1}^m A_k(\xi) a_k(\eta) B_k(\xi) b_k(\eta) C_k(\xi) c_k(\eta) \Omega_k(t). \end{aligned} \quad (21)$$

Multiplying equation (21) by $A_{hj}(\xi_h) a_{hj}(\eta_h) B_{hj}(\xi_h) b_{hj}(\eta_h) C_{hj}(\xi_h) c_{hj}(\eta_h)$ and performing integration,

$$\begin{aligned} \sum_{i=1}^{m_h} \int_0^1 \int_0^1 A_{hi}(\xi_h) a_{hi}(\eta_h) B_{hi}(\xi_h) b_{hi}(\eta_h) C_{hi}(\xi_h) c_{hi}(\eta_h) A_{hj}(\xi_h) a_{hj}(\eta_h) B_{hj}(\xi_h) b_{hj}(\eta_h) C_{hj}(\xi_h) c_{hj}(\eta_h) d\xi_h d\eta_h \Omega_{hj}(t) \\ = \sum_{k=1}^m \int_0^1 \int_0^1 A_{hi}(\xi_h) a_{hi}(\eta_h) B_{hi}(\xi_h) b_{hi}(\eta_h) C_{hi}(\xi_h) c_{hi}(\eta_h) A_k(\xi) a_k(\eta) B_k(\xi) b_k(\eta) C_k(\xi) c_k(\eta) d\xi_h d\eta_h \Omega_k(t). \end{aligned} \quad (22)$$

Using orthogonal property, equation (22) may be expressed as eigenfunctions of beam

$$\begin{aligned} &= \sum_{k=1}^m \int_0^1 A_{hi}(\xi_h) A_k(\xi) d\xi_h \int_0^1 a_{hi}(\eta_h) a_k(\eta) d\eta_h \int_0^1 B_{hi}(\xi_h) B_k(\xi) d\xi_h \\ &\int_0^1 b_{hi}(\eta_h) b_k(\eta) d\eta_h \int_0^1 C_{hi}(\xi_h) C_k(\xi) d\xi_h \int_0^1 c_{hi}(\eta_h) c_k(\eta) d\eta_h \Omega_k(t) \\ &= \sum_{k=1}^m (T_h)_{ik} \Omega_k(t), \quad i = 1, 2, 3, 4, \dots, m_h. \end{aligned} \quad (23)$$

If we write equation (23) as a matrix, we get

$$\Omega_h = T_{hi} \Omega, \quad (24)$$

matching requirement of the hole may be represented as follows:

$$\begin{aligned} w_h(\xi_h, \eta_h) &= w(\xi, \eta), \\ \psi_{hx}(\xi_h, \eta_h) &= \psi_x(\xi, \eta), \\ \psi_{hy}(\xi_h, \eta_h) &= \psi_y(\xi, \eta). \end{aligned} \quad (19)$$

The non-dimensional global and local coordinates have the following relationship:

$$\begin{aligned} \xi &= \frac{r_x}{a} + \frac{a_c}{a} \xi_h, \\ \eta &= \frac{r_y}{b} + \frac{b_c}{b} \eta_h. \end{aligned} \quad (20)$$

Considering equations (3), (10), (12), and (13) and by plugging them into equation (19), we can get

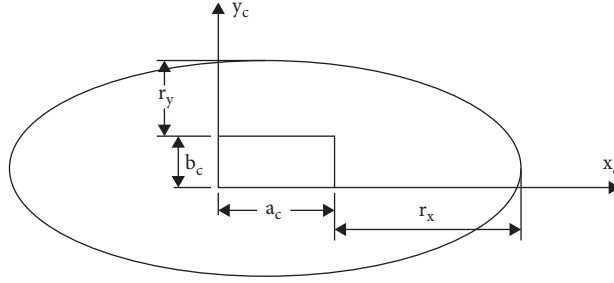


FIGURE 2: Elliptical plate with a rectangular cut-out.

in which T_h is the $m_h \times m$ matrix for transforming coordinates. Inserting equation (24) in to equations (15a) and (15b), we can derive

$$T_{\text{total}} = \frac{1}{2} \dot{\Omega}^T M \dot{\Omega} - \frac{1}{2} \dot{\Omega}^T T_h^T M_h T_h \dot{\Omega} = \frac{1}{2} \dot{\Omega}^T M_r \dot{\Omega}, \quad (25)$$

$$V_{\text{total}} = \frac{1}{2} \Omega^T K \Omega - \frac{1}{2} \Omega_h^T T_h^T K_h T_h \Omega_h = \frac{1}{2} \Omega^T K_r \Omega,$$

where $M_r = M - T_h^T M_h T_h$, $K_r = K - T_h^T K_h T_h$.

In non-dimensional parameters, equations can be stated.

$$M_r = \rho h b^2 \bar{M}_r, \quad (26a)$$

$$K_r = \frac{D}{b^2} \bar{K}_r,$$

$$\text{where } \bar{M}_r = \bar{M} - \left(\frac{\bar{b}_c^2}{b^2}\right) T_h^T \bar{M}_h T_h,$$

$$\bar{K}_r = \bar{K} - \left(\frac{1}{\bar{b}_c^2}\right) T_h^T \bar{K}_h T_h, \quad (26b)$$

in which $\bar{b}_{ci} = b_{ci}/b$ $i = 1, 2, 3, \dots, n$.

Hence,

$$[\bar{K}_r - \bar{\omega}^2 \bar{M}_r] \Lambda = 0. \quad (27)$$

From equation (23), ' T_h ' is the transformation matrix because of the integral limits. In equation (25), the eigenvalue of the plate with cut-out can be derived. Equation (26) is used to find the natural frequencies.

1.2. Free Vibrational Exploration of an Elliptical Plate Using ICCM. In the previous section, ICCM was used to evaluate a rectangular plate with a rectangular cut, where the plate and hole geometry were identical. In this section, the natural frequencies of an elliptical plate with a cut-out are computed using ICCM, with the hole and plate geometries modified. An elliptical plate with a hole is assumed in the plane. The semi-major axis "a" and semi-minor axis "b" are considered in direction. The border of an elliptical plate is written as $\xi^2 + \eta^2 = 1$.

The strain energy and kinetic energy of an elliptical plate is

$$V_p = \int_{\xi=0}^1 \int_{\eta=0}^{\sqrt{1-\xi^2}} \left\{ \left(\frac{1}{\alpha} \frac{\partial \psi_x}{\partial \xi} + \frac{\partial \psi_y}{\partial \eta} \right)^2 - 2(1-\mu) \left[\frac{1}{\alpha} \frac{\partial \psi_x}{\partial \xi} \frac{\partial \psi_y}{\partial \eta} - \frac{1}{4} \left(\frac{\partial \psi_x}{\partial \eta} + \frac{1}{\alpha} \frac{\partial \psi_y}{\partial \xi} \right)^2 \right] \right. \\ \left. + \frac{6(1-\mu)\kappa}{\beta^2} \left[\left(\psi_x + \frac{1}{\alpha} \frac{\partial w}{\partial \xi} \right)^2 + \left(\psi_y + \frac{\partial w}{\partial \eta} \right)^2 \right] \right\} ab d \xi d \eta, \quad (28)$$

$$T_p = \int_{\xi=0}^1 \int_{\eta=0}^{\sqrt{1-\xi^2}} \left[w^{*2} + \frac{1}{12} \beta^2 (\psi_x^2 + \psi_y^2) \right] ab d \xi d \eta.$$

Deflection and rotation terms in the energy expressions (26a) and (26b) of an elliptical plate, to get the non-dimensional parameters, may be written in terms of acceptable functions that are introduced in equation (3) of an elliptical plate. Using relationship between local and global coordinates of hole and plate in equation (20), transformation matrix can be derived by applying an orthogonal property on eigenfunctions. Reduced non-dimensional and elliptical plate with hole stiffness matrices with hole are obtained from equation (25). Equations (26a) and (26b) give the non-

dimensional eigenvalues of the plate with cut-out. Figure 2 shows the elliptical plate with a rectangular cut-out.

Table 1 shows the frequency parameter for a supported elliptical plate $a/b = 2$ and $h/b = 0.2$ of various sizes. Tables 2 and 3 show various sizes of $h/b = 0.4$ and $h/b = 0.6$.

1.3. Numerical Study. The ICCM is validated with the available literature for a rectangular plate with various aspect ratios and a thickness of $h/b = 0.2$ in Table 4. The current

TABLE 1: The frequency parameter, $\bar{\omega} = (\omega b^2/\pi^2)\sqrt{(\rho h/D)}$, for a simply supported elliptical plate $a/b = 2$, $h/b = 0.2$ of various sizes, $a_c/a = b_c/b = 0, 0.1, 0.2, 0.3, 0.4, 0.5, 0.6$.

$\bar{\omega}$	0	0.1	0.2	0.3	0.4	0.5	0.6
$\bar{\omega}_1$	0.3253	0.3129	0.2959	0.2889	0.2949	0.3145	0.3399
$\bar{\omega}_2$	0.5684	0.5662	0.5524	0.5312	0.5229	0.4819	0.4272
$\bar{\omega}_3$	0.8997	0.8927	0.8539	0.6602	0.5459	0.5419	0.5966
$\bar{\omega}_4$	1.0784	1.0427	0.9019	0.8999	0.8395	0.7653	0.7087
$\bar{\omega}_5$	1.3124	1.3003	1.2652	1.2487	1.1474	1.1067	1.1334
$\bar{\omega}_6$	1.4224	1.4026	1.3512	1.2959	1.3654	1.3101	1.2237

TABLE 2: The frequency parameter, $\bar{\omega} = (\omega b^2/\pi^2)\sqrt{(\rho h/D)}$, for a simply supported elliptical plate $a/b = 2$, $h/b = 0.4$ of various sizes, $a_c/a = b_c/b = 0, 0.1, 0.2, 0.3, 0.4, 0.5, 0.6$.

$\bar{\omega}$	0	0.1	0.2	0.3	0.4	0.5	0.6
$\bar{\omega}_1$	0.3043	0.2926	0.2761	0.2674	0.2677	0.2731	0.2636
$\bar{\omega}_2$	0.5096	0.5062	0.4902	0.4679	0.4377	0.3699	0.2972
$\bar{\omega}_3$	0.7724	0.7683	0.6883	0.5339	0.4562	0.4654	0.5002
$\bar{\omega}_4$	0.9099	0.8634	0.7714	0.7505	0.6786	0.6036	0.5544
$\bar{\omega}_5$	1.0776	1.0643	1.0387	1.0138	0.9216	0.8561	0.7968
$\bar{\omega}_6$	1.1531	1.1379	1.0987	1.0647	1.0865	0.9821	0.8469

TABLE 3: The frequency parameter, $\bar{\omega} = (\omega b^2/\pi^2)\sqrt{(\rho h/D)}$, for a simply supported elliptical plate $a/b = 2$, $h/b = 0.6$ of various sizes, $a_c/a = b_c/b = 0, 0.1, 0.2, 0.3, 0.4, 0.5, 0.6$.

$\bar{\omega}$	0	0.1	0.2	0.3	0.4	0.5	0.6
$\bar{\omega}_1$	0.2785	0.2685	0.2531	0.2427	0.2371	0.2296	0.2017
$\bar{\omega}_2$	0.4473	0.4431	0.4269	0.4058	0.3470	0.2823	0.2155
$\bar{\omega}_3$	0.6528	0.6509	0.5541	0.4296	0.3935	0.3964	0.4160
$\bar{\omega}_4$	0.7562	0.7066	0.6495	0.6171	0.5464	0.4831	0.4504
$\bar{\omega}_5$	0.8802	0.8673	0.8499	0.8199	0.7345	0.6549	0.5630
$\bar{\omega}_6$	0.9319	0.9212	0.8909	0.8715	0.8560	0.7395	0.5994

TABLE 4: Frequency parameter $\bar{\omega} = (\omega b^2/\pi^2)\sqrt{(\rho h/D)}$ of various aspect ratios having a plate thickness of $h/b = 0.2$.

Aspect ratio (a/b)	0.4	0.8	1	1.5	2
Present method	5.18318	2.20114	1.768	1.3164	1.15218
Ref. [1, 11]	5.1831	2.2011	1.7679	1.3164	1.1521
% error	—	—	—	—	—

TABLE 5: Frequency parameter $\bar{\omega} = (\omega b^2/\pi^2)\sqrt{(\rho h/D)}$ of a square plate with a cut-out thickness of $h = 0.2$.

	$a_c/a = b_c/b = 0.2$	$a_c/a = b_c/b = 0.4$	$a_c/a = b_c/b = 0.6$	$a/3 \times a/3$
Present method	1.718	1.8355	2.324	5137.428 (rad/sec)
Ref. [18]	1.716	1.8345	2.323	—
Ref. [6]	—	—	—	5136.5 (rad/sec)
% error	0.11%	0.054%	0.043%	0.02%

ICCM results seem to match the available data with a high degree of precision.

The results of a square plate with a cut-out of various sizes are validated with literature in Table 5.

From the Tables 4 and 5, it is clear that the improved ICCM produces correct results when compared to techniques such as RRM, FEM, and FDM, all of which have a

faster convergence time. As a result, the ICCM is used to find the natural frequencies of a thick rectangular plate with different aspect ratios and a cut-out elliptical plate by increasing the size of hole, in foregoing tables. Graphs are plotted in Figures 3 and 5 to show how these natural frequencies are varying with increase in size of cut-out for a rectangular plate and for an elliptical plate, respectively.

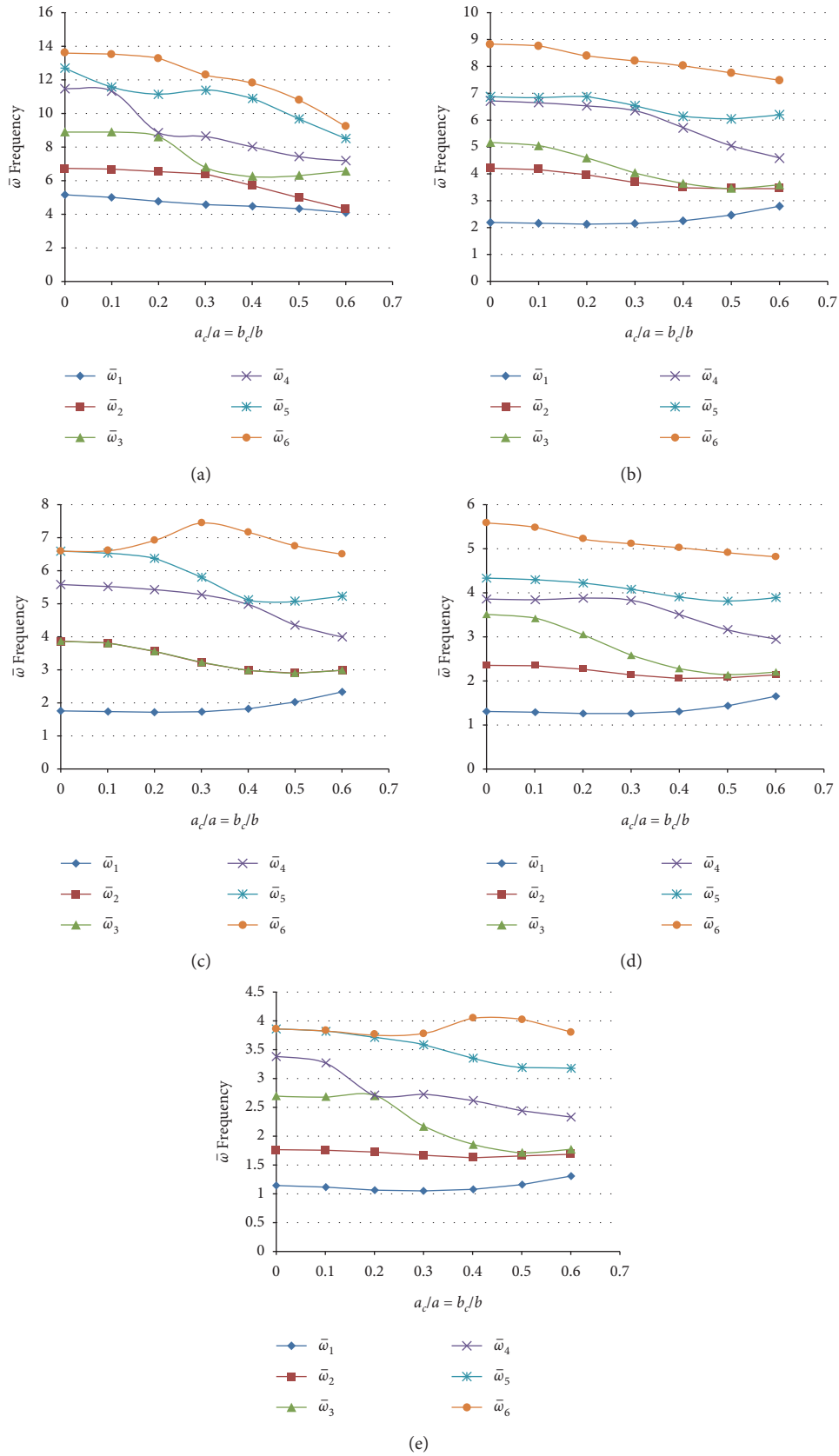
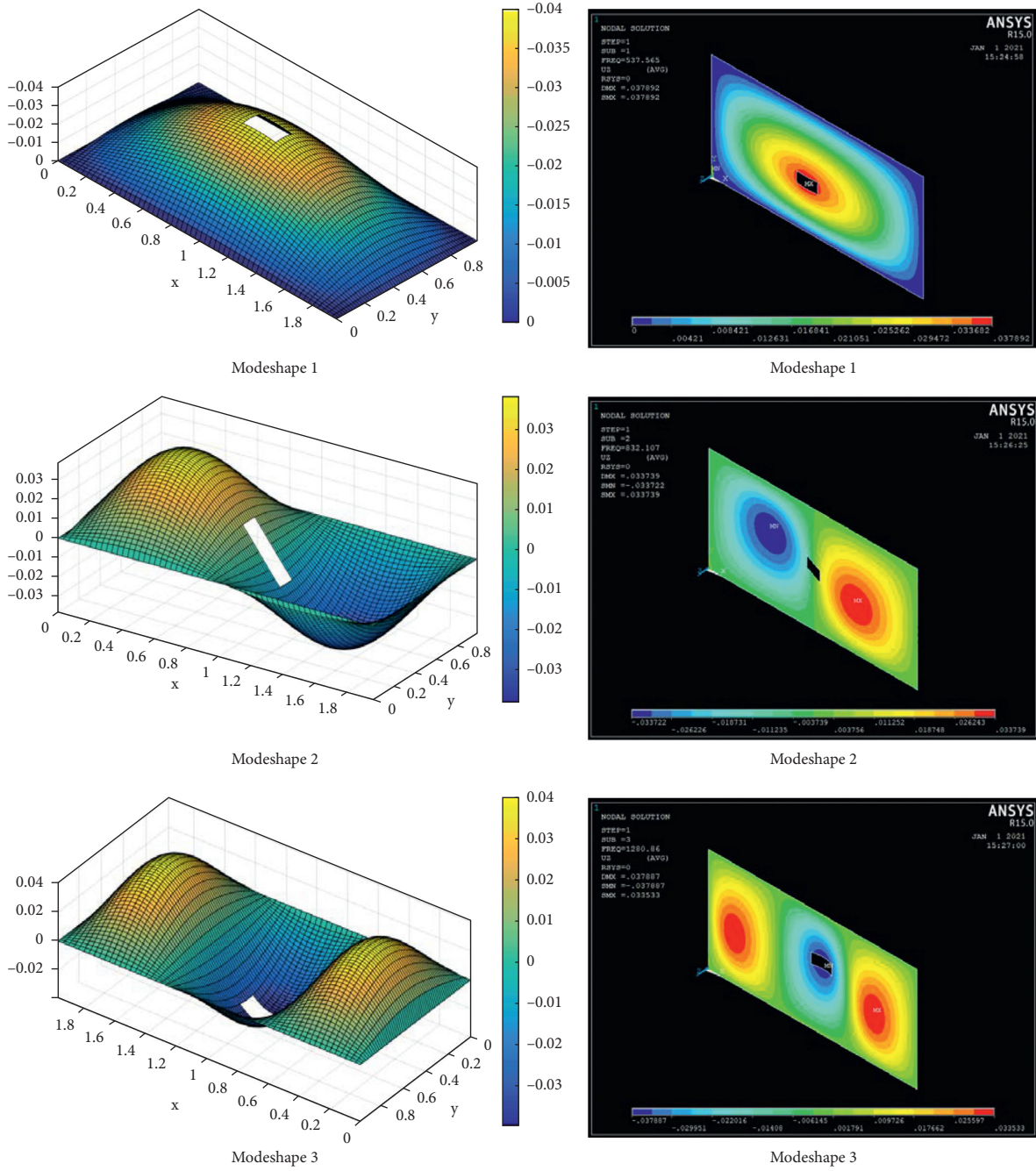


FIGURE 3: Aspect ratio variation of nondimensional eigenvalues. (a) Aspect ratio $a/b=0.4$ and $h/b=0.2$. (b) Aspect ratio $a/b=0.8$ and $h/b=0.2$. (c) Aspect ratio $a/b=1$ and $h/b=0.2$. (d) Aspect ratio $a/b=1.5$ and $h/b=0.2$. (e) Aspect ratio $a/b=2$ and $h/b=0.2$.



(a)

FIGURE 4: Continued.

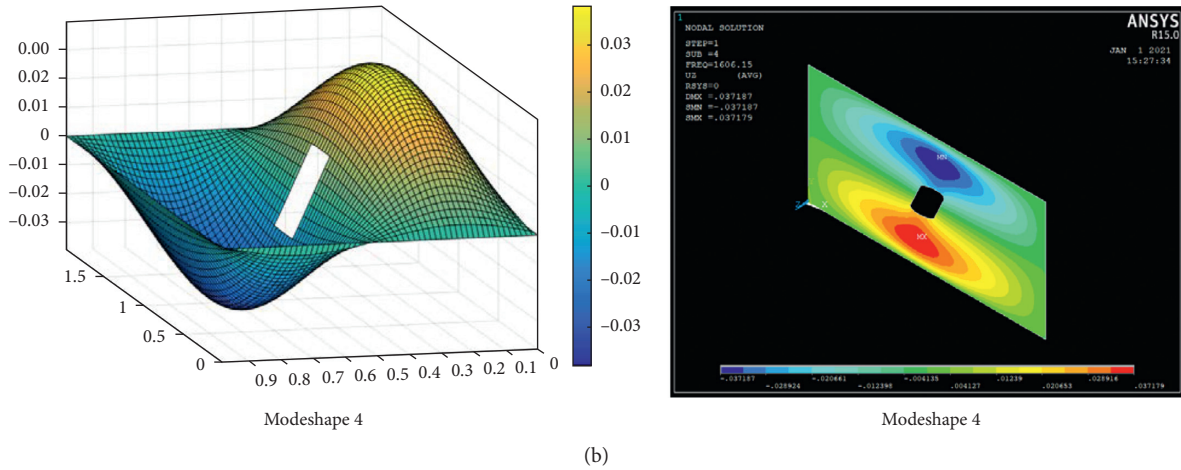


FIGURE 4: Comparison of transverse displacement of various mode shapes of a rectangular plate ($a = 2, b = 1$, and $h/b = 0.2$) with a concentric cut-out ($a_c/a = b_c/b = 0.1$) using MATLAB and ANSYS.

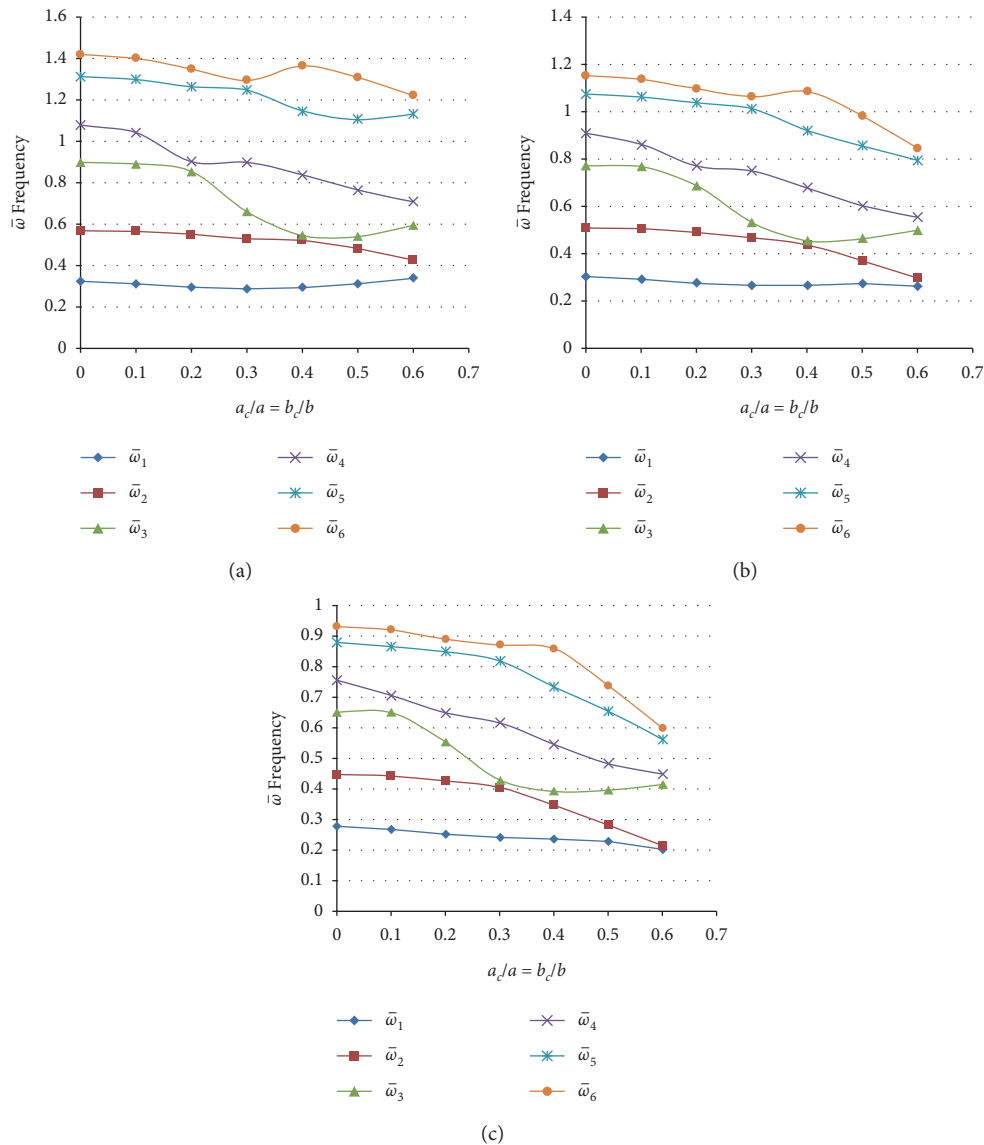


FIGURE 5: Variation of first six natural frequencies of an elliptical plate ($a/b = 2$) with respect to the size of cut-out. (a) Thickness ($h/b = 0.2$). (b) Thickness ($h/b = 0.4$). (c) Thickness ($h/b = 0.6$).

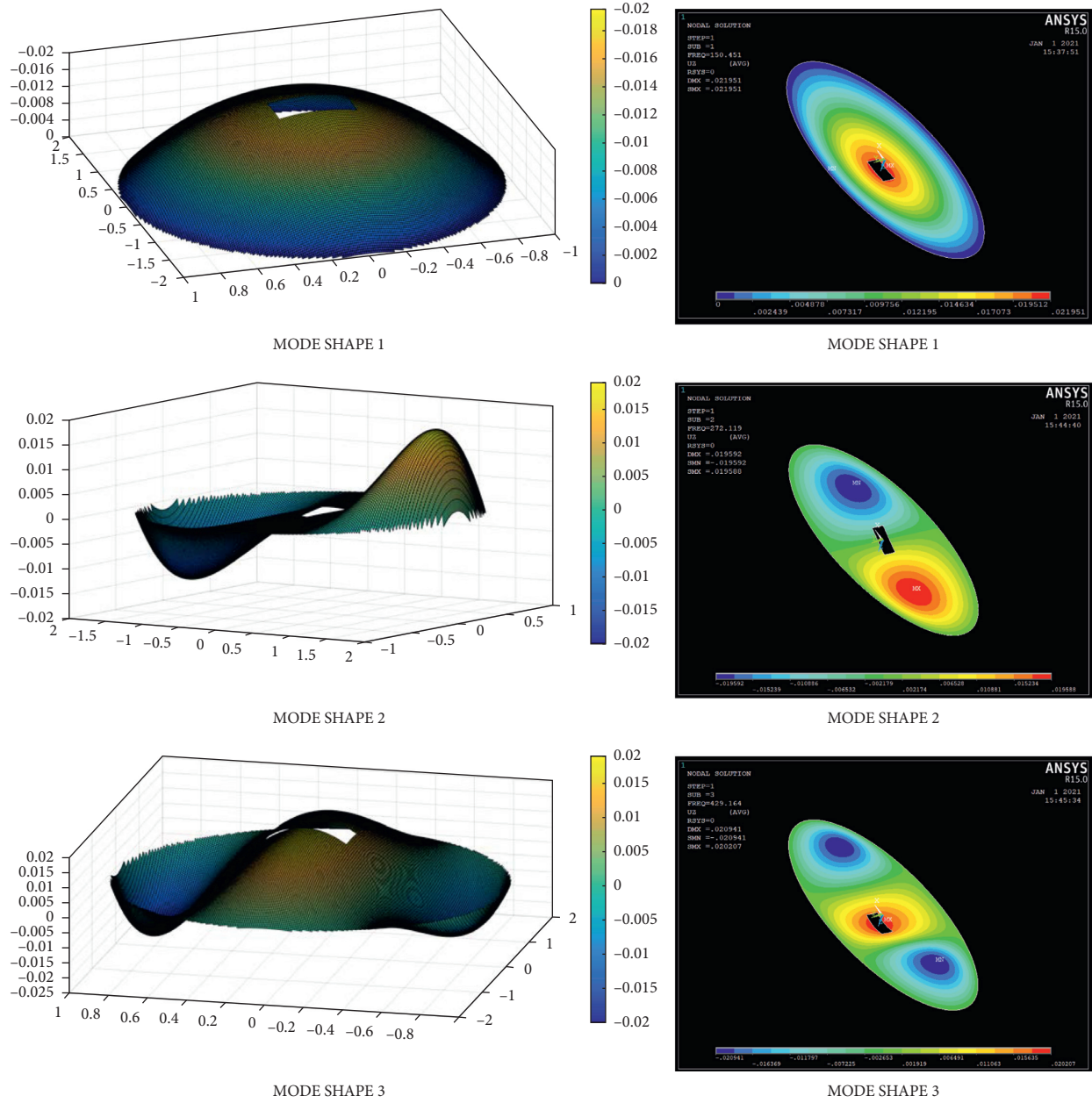


FIGURE 6: Comparison of transverse displacement of various mode shapes of an elliptical plate ($a = 2, b = 1,$ and $h/b = 0.2$) with a concentric cut-out ($a_c/a = b_c/b = 0.1$) using MATLAB and ANSYS.

TABLE 6: The frequency parameter, $\bar{\omega} = (\omega b^2/\pi^2)\sqrt{(\rho h/D)}$, for a simply supported rectangular plate with $a/b = 0.4$ and $h/b = 0.2$ with a concentric cut-out of various sizes, $a_c/a = b_c/b = 0, 0.1, 0.2, 0.3, 0.4, 0.5, 0.6$.

$\bar{\omega}$	0	0.1	0.2	0.3	0.4	0.5	0.6
$\bar{\omega}_1$	5.1831	5.0256	4.7675	4.5761	4.4598	4.3551	4.1113
$\bar{\omega}_2$	6.7212	6.6799	6.5428	6.3699	5.7165	4.9671	4.3116
$\bar{\omega}_3$	8.9138	8.8913	8.6299	6.7994	6.2705	6.3248	6.5839
$\bar{\omega}_4$	11.4875	11.3366	8.8808	8.6475	8.0246	7.4310	7.2052
$\bar{\omega}_5$	12.7040	11.5864	11.1545	11.4103	10.8954	9.6713	8.5177
$\bar{\omega}_6$	13.6145	13.5469	13.2805	12.3054	11.8309	10.799	9.2534

TABLE 7: The frequency parameter, $\bar{\omega} = (\omega b^2/\pi^2)\sqrt{(\rho h/D)}$, for a simply supported rectangular plate with $a/b = 0.8$ and $h/b = 0.2$ with a concentric cut-out of various sizes, $a_c/a = b_c/b = 0, 0.1, 0.2, 0.3, 0.4, 0.5, 0.6$.

$\bar{\omega}$	0	0.1	0.2	0.3	0.4	0.5	0.6
$\bar{\omega}_1$	2.2011	2.1688	2.1314	2.1517	2.2574	2.4669	2.7971
$\bar{\omega}_2$	4.2113	4.1600	3.9625	3.6882	3.4964	3.4614	3.4616
$\bar{\omega}_3$	5.1831	5.0662	4.6087	4.0433	3.6548	3.4749	3.6022
$\bar{\omega}_4$	6.7212	6.6538	6.5398	6.3630	5.7270	5.0472	4.6080
$\bar{\omega}_5$	6.8703	6.8504	6.8794	6.5353	6.1591	6.0669	6.2075
$\bar{\omega}_6$	8.8381	8.7715	8.3998	8.2281	8.0359	7.7668	7.4985

TABLE 8: Frequency parameter for supported elliptical plate with $a/b = 1$ and $h/b = 0.2$.

$\bar{\omega}$	0	0.1	0.2	0.3	0.4	0.5	0.6
$\bar{\omega}_1$	1.7680	1.7446	1.7180	1.7402	1.8355	2.0222	2.3245
$\bar{\omega}_2$	3.8667	3.8089	3.5668	3.2336	2.9938	2.9118	2.9903
$\bar{\omega}_3$	3.8667	3.8093	3.5674	3.2342	2.9941	2.9121	2.9905
$\bar{\omega}_4$	5.5892	5.5317	5.4308	5.2881	4.9846	4.3669	3.9942
$\bar{\omega}_5$	6.6046	6.5418	6.3772	5.8040	5.1319	5.0782	5.2457
$\bar{\omega}_6$	6.6046	6.6107	6.9262	7.4488	7.1699	6.7593	6.5139

TABLE 9: Frequency parameter for supported elliptical plate with $a/b = 1.5$ and $h/b = 0.2$.

$\bar{\omega}$	0	0.1	0.2	0.3	0.4	0.5	0.6
$\bar{\omega}_1$	1.3164	1.2892	1.2549	1.2577	1.3146	1.4388	1.6507
$\bar{\omega}_2$	2.3612	2.3441	2.2673	2.1496	2.0686	2.0764	2.1431
$\bar{\omega}_3$	3.5119	3.4285	3.0505	2.5884	2.2852	2.1470	2.2043
$\bar{\omega}_4$	3.8659	3.8465	3.8823	3.8363	3.5104	3.1620	2.9547
$\bar{\omega}_5$	4.3406	4.2991	4.2203	4.0807	3.9096	3.8168	3.8947
$\bar{\omega}_6$	5.5881	5.4895	5.2256	5.1161	5.0262	4.9138	4.8277

TABLE 10: Frequency parameter for supported elliptical plate with $a/b = 2$ and $h/b = 0.2$.

$\bar{\omega}$	0	0.1	0.2	0.3	0.4	0.5	0.6
$\bar{\omega}_1$	1.1521	1.1167	1.0688	1.0528	1.0810	1.1622	1.3106
$\bar{\omega}_2$	1.7680	1.7606	1.7244	1.6674	1.6338	1.6604	1.6913
$\bar{\omega}_3$	2.7027	2.6848	2.7079	2.1736	1.8632	1.7208	1.7764
$\bar{\omega}_4$	3.3858	3.2700	2.7181	2.7295	2.6171	2.4452	2.3393
$\bar{\omega}_5$	3.8667	3.8222	3.7156	3.5897	3.3512	3.1934	3.1870
$\bar{\omega}_6$	3.8667	3.8378	3.7652	3.7843	4.0480	4.0253	3.8016

TABLE 11: Various aspect ratios of plate.

Aspect ratio a/b	h/b	Cut-out size at which lowest ω is obtained $a_c/a = b_c/b =$	% of ω reduced, when compared with a plate without cut-out
0.4	0.2	0.6	20.6
0.8	0.2	0.2	3.16
1	0.2	0.2	2.82
1.5	0.2	0.2	4.67
2	0.2	0.3	8.61

TABLE 12: Various thickness ratios of plate.

Aspect ratio (a/b)	h/b	Cut-out size at which lowest ω is obtained $a_c/a = b_c/b$	% of ω reduced, when compared with a plate without cut-out
2	0.2	0.3	11.18
2	0.4	0.6	13.37
2	0.6	0.6	27.57

Eigenvectors were also plotted to observe the deflection in Z-direction for each mode of vibration, and it is validated with the mode shape obtained from ANSYS in Figures 4 and 6.

Graphs were plotted for a numerical value in Tables 6–10, as a function of cut-out size.

Case 1. Rectangular plate of different aspect ratios with concentric rectangular hole with increase in its size.

Case 2. An elliptical plate of aspect ratio ($a/b = 2$) of various thickness having a concentric rectangular hole with increase in its size.

2. Results and Discussion

This paper delves at the first six natural frequencies of a thick, rectangular, and elliptical plate. A cut-out is derived using ICCM. Based on the various combinations of aspect ratios and cut-out sizes, the derived numerical results were plotted in Figures 3 and 5. The frequency occurs due to a large hole, and maximum variation was observed compared to a plate without a cut. These observations were tabulated as follows so that the designers can change the natural frequency of a structure up to maximum limit of scope simply by introducing a cut-out. Figure 6 shows the comparison of transverse displacement of various mode shapes of an elliptical plate.

2.1. Rectangular Plate with Cut-Out. The eigenvalue of a rectangular plate with a hole is lower when compared to a rectangular plate without a cut-out, as seen in the images. For an aspect ratio of $a/b = 0.4$ and $h/b = 0.2$, the lowest natural frequency is obtained with a cut-out of size $a_c/a = b_c/b = 0.6$. The cut-out frequency is reduced by 20.6%. Similarly, rectangular plates with cut-out frequency are increased. The combination of aspect ratios and cut-outs are as shown in Table 11.

2.2. Elliptical Plate with Cut-Out. For an aspect ratio of $a/b = 2$ and $h/b = 0.2$, the lowest natural frequency is obtained with a cut-out of size $a_c/a = b_c/b = 0.3$. The frequency is reduced by 11.18% when compared to other combinations of thickness ratios and cut-outs. The lowest natural frequency is obtained as shown in Table 12.

This information is useful to the designers to vary the natural frequency of a structure, up to a maximum limit of scope simply by introducing a cut-out.

3. Conclusions

Numerical results, plotted as curves in Figure 3, reveal that as aspect ratio of the plate is increased, natural frequencies were decreased due to increase in mass without a significant increase in stiffness and the behavior of fundamental natural frequency is consistent with the variation of size of cut-out. It is also observed that in every aspect ratio, 2nd and 3rd mode of frequencies can be made same by including an appropriate size of cut-out. In the same manner, 4th and 5th mode of frequencies can also be made same in every aspect ratio of plate. Aspect ratio $a/b = 0.8$ with $h/b = 0.2$ has a high-frequency range that significantly increased the mass compared to aspect ratio 1. Due to the change in stiffness, the variation of frequencies exists that is smooth in manner. From Figure 5, it is worth noting that increasing the thickness ratio has no discernible influence on the plate's basic natural frequency. In every thickness ratio, mode 3 natural frequency can be made equal to mode 2 natural frequency by introducing a cut-out of size nearer to 0.4, and hence by introducing a cut-out, structure can be made to vibrate in different modes for the same value of natural frequency. From the analysis, for the study of a thick plate with cut-outs, modified ICCM is an excellent numerical tool that converges to the solution faster than other traditional approaches.

Data Availability

The data used to support the findings of this study are included within the article.

Disclosure

This research was performed as a part of the employment of Mettu University, Ethiopia.

Conflicts of Interest

The authors declare that there are no conflicts of interest regarding the publication of this paper.

Acknowledgments

The authors thank Aditya College of Engineering, Andhra Pradesh, University College of Engineering, JNTUK, Kakinada, and Saveetha School of Engineering, SIMATS, Chennai, for the technical assistance. The authors also appreciate the support from Mettu University, Ethiopia.

References

- [1] I. Senjanovic, N. Vladimir, and M. Tomic, "An Advanced Theory of moderately thick plate vibrations," *Journal of Sound and Vibration*, vol. 332, no. 7, pp. 1868–1880, 2013.
- [2] I. Senjanović, M. Tomić, N. Vladimir, and D. S. Cho, "Analytical solution for free vibrations of a moderately thick rectangular plate," *Mathematical Problems in Engineering*, vol. 2013, Article ID 207460, 13 pages, 2013.
- [3] Y. Xiang, S. K. Lai, and L. Zhou, "DSC-element method for free vibration analysis of rectangular mindlin plates," *International Journal of Mechanical Sciences*, vol. 52, no. 4, pp. 548–560, 2010.
- [4] A. Merneedi, M. R. Nalluri, and V. S. R. Vissakodeti, "Free vibration analysis of an elliptical plate with cut-out," *Journal of Vibroengineering*, vol. 19, no. 4, pp. 2341–2353, 2017.
- [5] A. Merneedi, M. RaoNalluri, and V. V. S. Rao, "Free vibration analysis of a thin rectangular plate with multiple circular and rectangular cut-outs," *Journal of Mechanical Science and Technology*, vol. 31, no. 11, pp. 5185–5202, 2017.
- [6] G. Aksu, "Free vibration analysis of rectangular plates with cutouts allowing for transverse shear deformation and rotary inertia," *Earthquake Engineering & Structural Dynamics*, vol. 12, no. 5, pp. 709–714, 1984.
- [7] L. Rui, P. Wang, X. Riye, and G. Xu, "New analytical solutions for free vibration of rectangular thick plates with an edge free," *International Journal of Mechanical Sciences*, vol. 131–132, pp. 179–190, 2017.
- [8] Y. Xing and B. Liu, "Closed form solutions for free vibrations of rectangular mindlin plates," *The Chinese society of theoretical and applied mechanics and springer*, vol. 25, pp. 689–698, 2009.
- [9] Y. Xing and B. Liu, "Characteristic equations and closed-form solutions for free vibrations of rectangular Mindlin plates," *Acta Mechanica Sinica*, vol. 22, no. 2, pp. 125–136, 2009.
- [10] K. M. Liew, K. C. Hung, and M. K. Lim, "Vibration of Mindlin plates using boundary characteristic orthogonal polynomials," *Journal of Sound and Vibration*, vol. 182, no. 1, pp. 77–90, 1995.
- [11] K. M. Liew, Y. Xiang, and S. Kitipornchai, "Transverse vibration of thick rectangular plates-I. Comprehensive sets of boundary conditions," *Computers & Structures*, vol. 49, no. 1, pp. 1–29, 1993.
- [12] K. M. Liew, K. C. Hung, and M. K. Lim, "A continuum three-dimensional vibration analysis of thick rectangular plates," *International Journal of Solids and Structures*, vol. 30, no. 24, pp. 3357–3379, 1993.
- [13] C. W. Lim, K. M. Liew, and S. Kitipornchai, "Numerical aspects for free vibration of thick plates part I: formulation and verification," *Computer Methods in Applied Mechanics and Engineering*, vol. 156, no. 1-4, pp. 15–29, 1998.
- [14] D. J. Dawe and O. L. Roufaeil, "Rayleigh-Ritz vibration analysis of Mindlin plates," *Journal of Sound and Vibration*, vol. 69, no. 3, pp. 345–359, 1980.
- [15] A. W. Leissa, "The free vibration of rectangular plates," *Journal of Sound and Vibration*, vol. 31, no. 3, pp. 257–293, 1973.
- [16] N. F. Hanna and A. W. Leissa, "A higher order shear deformation theory for the vibration of thick plates," *Journal of Sound and Vibration*, vol. 170, no. 4, pp. 545–555, 1994.
- [17] A. S. sayyad and Y. M Ghugal, "Bending and free vibration analysis of thick isotropic plates by using exponential shear deformation theory," *Applied and computational mechanics*, vol. 6, pp. 65–82, 2012.
- [18] K. Kanak and H. Salil, "Free vibration analysis of rectangular plates with central cut-out," *Cogent Engineering*, vol. 3, no. 1, p. 12, 2016.
- [19] K. L. Prasad, A. Venkateshwar Rao, and B. Nageswara Rao, "Free vibration of simply supported and clamped elliptical plates," *Journal of Sound and Vibration*, vol. 158, no. 2, pp. 383–386, 1992.
- [20] A. W. Leissa, "Vibration of a simply-supported elliptical plate," *Journal of Sound and Vibration*, vol. 6, no. 1, pp. 145–148, 1967.
- [21] M. J. Maurizi, P. Belles, and P. A. A. Laura, "Free vibration of clamped elliptical plates," *Journal of Sound and Vibration*, vol. 171, no. 1, pp. 141–144, 1994.
- [22] K. Y. Lam, K. M. Liew, and S. T. Chow, "Use of two-dimensional orthogonal polynomials for vibration analysis of circular and elliptical plates," *Journal of Sound and Vibration*, vol. 154, no. 2, pp. 261–269, 1992.
- [23] Y. Shibaoka, "On the transverse vibration of an elliptic plate with clamped edge," *Journal of the Physical Society of Japan*, vol. 11, no. 7, pp. 797–803, 1956.
- [24] R. P. Mcnitt, "Free vibration of a damped elliptical plate," *Journal of the Aerospace Sciences*, vol. 29, no. 9, pp. 1124–1125, 1962.
- [25] M. K. Kwak and S. Han, "Free vibration analysis of rectangular plate with a hole by means of Independent coordinate coupling method," *Journal of Sound and Vibration*, vol. 306, no. 1-2, pp. 12–30, 2007.
- [26] S. M. Hasheminejad, A. Ghaheri, and SajjadVaezian, "Exact solution for free vibration analysis of an eccentric elliptical plate," *Archive of Applied Mechanics*, vol. 84, no. 4, pp. 543–552, 2014.
- [27] L. Natarayan and A. Merneedi, "Experimental investigation on wear behaviour of bio-waste reinforced fusion fiber composite laminate under various conditions," *Materials Today: Proceedings*, vol. 37, no. 2, pp. 1486–1490, 2021.